Desalination and Water Treatment
www.deswater.com

doi:10.5004/dwt.2017.20646

79 (2017) 251–263
June

Application of superparamagnetic polymer-coated magnetite nanoparticles for non-competitive removal of Cd(II) and Zn(II) from aqueous solutions

Hamid Ershadifar[a], Morteza Akhond[b], Ghodratollah Absalan[b,*]

[a]*Current address: Iranian National Institute for Oceanography and Atmospheric Science (INIOAS), P.O. Box 14155-4781, Tehran, Iran, email: Ershadifar.hamid@yahoo.com (H. Ershadifar), Akhond@susc.ac.ir (M. Akhond)*
[b]*Professor Massoumi Laboratory, Department of Chemistry, College of Sciences, Shiraz University, Shiraz, 71454, Iran, Tel. +98 (71)3613-7137, Fax +98 (71)3646-0788, email address: gubsulun@yahoo.com; absalan@susc.ac.ir (G. Absalan)*

Received 16 June 2016; Accepted 2 March 2017

ABSTRACT

Magnetic nanoparticles modified with cross-linked poly (acrylic acid-co-acrylamide) hydrogel (Fe_3O_4/copolymer) were fabricated by free radical polymerization of monomers in the presence of N, N-methylenebisacrylamide as cross-linker and dispersed Fe_3O_4 nanoparticles as core. The Fe_3O_4/copolymer composite was characterized by Fourier transform infrared spectrum (FT-IR), scanning electron microscopy (SEM), X-ray diffraction (XRD), thermal gravimetric analysis (TGA), and vibrating sample magnetometer (VSM). The fabricated magnetic nanocomposites were further utilized for non-competitive removal of Cd(II) and Zn(II). The adsorbent component, adsorbent dosage, concentration of the initial solute, and the pH of the solution were found to have significant effects on adsorption efficiency. The adsorption process was found to be well described by the pseudo-second-order rate model. Equilibrium studies indicated that the adsorption data followed the Langmuir model with the maximum adsorption capacity up to 142.8 and 111.1 mg/g for Cd(II) and Zn(II), respectively. Adsorbed metal ions were efficiently recovered by using a dilute HCl aqueous solution. The results of desorption/adsorption cycle revealed that the loaded Fe_3O_4/copolymer nanocomposite with metal ions could be effectively regenerated. Adsorption capacities and metal ions recoveries remained almost unchanged upon five reusing cycles of the adsorbent.

Keywords: Magnetic nanoparticles; Hydrogel polymer; Adsorption; Zinc; Cadmium

1. Introduction

As industrial and ecological waste problems are increasing, the removal of heavy metal ions from wastewater samples has taken much important attention. The two important toxic metal ions are cadmium and zinc which their presence in wastewaters originates from different industrial activities such as paint production [1], battery manufacturing [2], petroleum refining [3] and from pesticides [4]. Cadmium has been reported to cause renal disturbances, lung insufficiency, bone lesions, cancer and hypertension in humans [5]. The concentrations of Cd(II) in unpolluted natural waters are usually below 0.001 mg L^{-1} [6]; therefore, it is necessary to remove it from industrial effluents. However, World Health Organization (WHO) has recommended a value of 0.005 mg L^{-1} for Cd(II) as maximum permissible limit [7]. Concerning zinc, WHO recommends that the maximum acceptable concentration of zinc in drinking water is 3 mg L^{-1} [8]. Exposure to Zn(II) can lead to stomach cramps, skin irritations, vomiting, nausea and anemia [9].

Adsorption techniques are among the most effective treatment processes for the removal of heavy metal ions from aquatic environment. Unlike traditional methods, which are relatively expensive and require particular treatments especially at low concentration levels of the metal ions [10], the adsorption techniques are efficiently and widely chosen

*Corresponding author.

for water treatment purposes and have many advantages such as low cost, availability, and ease of operation. However, attempts are still required to develop new adsorbents because the common adsorbents such as activated carbons, zeolites, clays, biomass, and polymeric materials [11] suffer from low adsorption capacities and separation inconveniency. A lot of materials such as hydroxyapatite [12], biosorbents [13], polymer beads [14], aminopolycarboxylic acid functionalized adsorbents [15], β-cyclodextrin/chitosan composites [16], mesoporous carbon [17], magnetic graphene oxide nanocomposites [18] and polymeric materials [19] are well-known for efficient removal of heavy metal ions from aqueous solutions.

In recent years, reusable magnetic adsorbents in nanometer and micrometer sizes have attracted much attention due to fast and efficient removal of heavy metals from aqueous samples under an applied magnetic field. However, it should be pointed out that the pure metal oxides nanoparticles are neither selective nor chemically stable, i.e, they are not suitable for samples with complicated matrices especially in acidic media [20]. Therefore, a suitable coating technique is required to overcome such limitations. In this regard, magnetic nanocomposites modified with polymers [21–23], surfactants [24], and silica [25,26] have been proposed for removal of organic pollutant as well as heavy metal ions from aqueous media. Among them, polymer-functionalized Fe_3O_4 nano- and micro-composites which can be fabricated in different shapes are of great importance. A considerable advantage of the polymeric carriers is the presence of a variety of functional groups, which are able to manipulate the sorbent properties for the desired applications.

Hydrogels are water-swollen cross-linked networks of hydrophilic polymers. Due to the hydrophilic groups (carboxylic and amide) in their backbones, they can absorb a large amount of water and consequently are able to remove metal ions including the toxic ones from aqueous media [27]. So far, various strategies have been proposed for synthesis of magnetic polymer particles. Khan et al. [28] prepared and characterized magnetic nanoparticles embedded in microgels. Guo et al. [29] has prepared and characterized poly (acrylonitrile-co-acrylic acid) nanofibrous composites with Fe_3O_4 magnetic nanoparticles. Mahdavian et al. [30] has fabricated modified superparamagnetic magnetite nanoparticles by anchoring polyacrylic acid on their surface for efficient separation of heavy metal cations from aqueous environments. Although the reported researches on the removal of metal ions fulfill some requirements but fabrication of sorbents with low cost, high capacity, short equilibrium time, facile and environmentally friendly fabrication route and applicable in wide pH range is still of great demand.

This paper describes a general method to encapsulate magnetic nanoparticles homogeneously inside a polymer shell. Characterization of the composite has been done using a variety of physicochemical techniques. The main goal of this research was to evaluate the sorption behavior of Cd(II) and Zn(II) onto Fe_3O_4/polymer and to compare the performance of Fe_3O_4/polymer adsorbents with those of other adsorbents. Some factors affecting the adsorption of these metal ions, such as pH, initial concentration, contact time and temperature were investigated. The relevant removal mechanisms of metal ions onto Fe_3O_4/polymer were well expounded via adsorption kinetics, isotherms and thermodynamics. Regeneration and reusability were also examined for further application of this new type of adsorbent to more complex water environment.

2. Experimental

2.1. Chemicals and reagents

Acrylic acid (AAc, Fluka), acrylamide (AAm, Merk), N,N-methylenebisacrylamide (MBA, Merk), potassium persulfate ($K_2S_2O_8$, Merk), and sodium thiosulfate ($Na_2S_2O_3$, Merk), were used as received from the indicated suppliers. In the preparation of magnetite nanoparticles, ferrous chloride hexahydrate ($FeCl_3{\cdot}6H_2O$, Merk), ferric sulphate heptahydrate ($FeSO_4{\cdot}7H_2O$, Merk) and sodium hydroxide (Merk) were used. Cadmium nitrate ($Cd(NO_3)_2{\cdot}4H_2O$, Merk), zinc nitrate hexahydrate ($Zn(NO_3)_2{\cdot}6H_2O$, Merk), hydrochloric acid (Sigma-Aldrich), and nirtic acid (Merk) were used in adsorption experiments. The stock solutions (1000 mg L^{-1}) were of Cd(II) and Zn(II). For treatment experiments, the metal ions solutions with concentrations in the range of 0.1–500 mg L^{-1} were prepared by successive dilution of the corresponding stock solution. The pH adjustment was performed with HNO_3 and NaOH solutions (0.01–1.0 mol L^{-1}). All aqueous solutions were prepared or diluted using doubly distilled water.

2.2. Synthesis of magnetic nanoparticles

The magnetic nanoparticles of iron oxide (Fe_3O_4NP) were synthesized by dropwise addition of a mixture of ferrous sulfate and ferric chloride (mol ratio of 1:2) solution into NaOH solution (1.5 mol L^{-1}) with constant stirring under argon gas flow [31]. The black precipitate was heated at 80°C for 30 min and was sonicated for 20 min afterward. Then, it was washed sequentially with distilled water until the pH of the suspension was about 8.0. The precipitate was separated magnetically and was dried in an oven for further analysis.

2.3. Synthesis of magnetic hydrogel

Synthesis of Fe_3O_4/polymer has been performed with the aid of previously reported methods for cross-linked poly (AAc-co-AAm) hydrogel with applying some modifications as discussed below [32]. Briefly, 0.5 g of the magnetite nanoparticles was dispersed in 10.0 mL distilled water and was sonicated for 30 min. The surface of Fe_3O_4 NPs was grafted with acrylic acid by the following procedure. Aliquot of 5.0 mL of 1.0 mol L^{-1} acrylic acid (75%; neutralized to sodium acrylate) was added to the above mentioned suspension. The mixture was shaken at a rate of 450 rpm for 1 h. The acrylic acid monomers were anchored at the surface of Fe_3O_4 by a simple complexation reaction with unsaturated iron ions at the nanoparticle surface. Then, a predetermined amount of cross-linking agent was introduced into a 50.0 mL beaker, followed by adding a predetermined volume of 1.0 M acrylamide solution into the beaker. Oxygen was purged out of the solution by

bubbling pure argon gas through the solution for 10 min at room temperature while the solution was stirred at 450 rpm. Subsequently, 1.0 mL of the initiator (0.1 M potassium persulfate) solution was injected into the beaker. Then, 1.0 mL of 0.1 M accelerator (sodium thiosulfate) was added into the solution, followed by nitrogen gas purging for 5 min. The beaker was enclosed into a plastic bag filled with pure argon gas for blanketing the reaction mixture. After polymerization, a dark magnetite-hydrogel composite formed. For complete polymerization, the beaker was kept in an oven at 45°C for about 1 h. The magnetite-hydrogel composite was broken into smaller sizes and immersed in deionized water while stirring for 5 h to remove the residual monomers and linear copolymers. The composite was then dried in an oven at 60–80°C and eventually further dried under vacuum at 60–80°C until a constant weight of the sample was established.

2.4. Batch experiments

Metal ion-removal ability of the synthesized Fe_3O_4/polymer was performed by using batch technique for individual metal ion based on a procedure described as follows. Known masses (2.0–40.0 mg) of the adsorbent were weighed and individually introduced into a series of 20-mL beakers containing 10 mL of the metal solution at specific concentration (0.1–300 mg L^{-1}). The initial pH of the solutions was adjusted at 6.0 using HNO_3 or NaOH. The solutions were stirred for 5 min at 450 rpm to attain the equilibrium condition. After adsorption time elapsed, the adsorbent was magnetically separated and the supernatant was collected for metal ions measurement. The residual concentration of each metal ion in the solution was determined by ICP-OES. The amounts of the adsorbed metal ions at equilibrium and at the time t were obtained by using Eqs. (1) and (2), respectively.

$$q_e = \frac{V(C_0 - C_e)}{W} \quad (1)$$

$$q_t = \frac{V(C_0 - C_t)}{W} \quad (2)$$

where q_e (in mg g^{-1}) is the adsorption capacity (mg metal ion adsorbed per gram Fe_3O_4/polymer), V (in Liter) is the volume of metal ion solution, C_0 and C_e are the initial and equilibrium metal ion concentrations (in mg L^{-1}), respectively; C_t and q_t referred to metal ion concentration and adsorption capacity at adsorption time t, in order; and W is the mass (in g) of the dried Fe_3O_4 /polymer.

For real sample analysis, tap water was collected from our laboratory (Date: 2014/07/05, Department of Chemistry, Shiraz University, Fars, Iran). Mineral waters (Vivante, Nousha Zagros Manufacturing Co., Shiraz, Iran) were supplied from a local supermarket and were used without any pretreatment except adjusting the pH at 6.0 using HNO_3 or NaOH.

2.5. Apparatus

The concentrations of Zn(II) and Cd(II) were determined by a Vista-PRO ICP-OES (Varian). The surface group of the composite was recorded on a Shimadzu FTIR 8000 spectrometer; small amounts of the solid nanoparticles were mixed with KBr and pressed into pellets. The FTIR spectra were recorded from 400 to 4000 cm^{-1} in the transmittance mode. The XRD patterns of the prepared samples were acquired with a Bruker D8 instrument. Advance X-ray diffractometer using CuK_α radiation (40 kV, 300 mA) of wavelength 0.154 nm was used and data were interpreted by using an X'Pert High Score software to confirm the structure of the materials. Thermogravimetric analysis (TGA) was carried out using a home-made TG analyzer, with a heating rate of 10°C min^{-1} from room temperature to 800°C. The surface morphological characterization of the composites was studied with a KYKY-EM3200 SEM, operating at 25.0 kV. The magnetic properties of the nanoparticles were measured on a BHV-55 vibrating sample magnetometer (VSM). The pH measurements were made with a Metrohm 780 pH meter using a combined glass electrode.

2.6. pH drift tests

The pH drift tests for modified and unmodified magnetite nanoparticles were carried out at 298 K as follows: 50.0 mL of 0.1 M NaCl solution was placed in a beaker. Argon was bubbled through the solution to stabilize the pH by preventing the dissolution of CO_2. The pH was adjusted to a value between 2.0 and 12.0 by addition of HCl or NaOH. The adsorbent (0.1 g) was added to the solution and its final pH was measured after 48 h which was then plotted against the initial pH. The pH at which the curve crossed the line (in $pH_{initial}$ *vs.* pH_{final} diagram) was taken as the point of zero charge, pH_{PZC}.

2.7. Desorption studies

The adsorption-desorption tests were conducted in batch adsorption-equilibrium experiments to evaluate the regeneration behavior of Fe_3O_4/polymer nanocomposite. A mass of 10.0 mg adsorbent was introduced into a beaker containing 10.0 mL of 40.0 mg L^{-1} metal ion. The solution was stirred for 5 min to attain the equilibrium condition. The supernatant was separated for determination of the residual concentration of the metal ion and the collected magnetic nanocomposites were used for desorbing the metal ions. To do the later, the metal ion-loaded magnetic nanocomposites were mixed with 0.01 M HCl and the mixture was stirred at 450 rpm for 10 min at room temperature and eventually the desorbed metal ion concentration in the aqueous phase was determined. The amount of the desorbed metal ion divided by the amount of the adsorbed metal ions give the recovered fraction of the metal ion.

3. Results and discussion

3.1. Protocol for synthesis of Fe_3O_4/polymer nanocomposite

The procedure for synthesize of Fe_3O_4/polymer nanocomposite is illustrated schematically in Fig.1. This ensures the homogenous copolymerization process for formation of the cross-linked hydrogel shell around nanoparticles to improve stability and adsorption performance of the adsor-

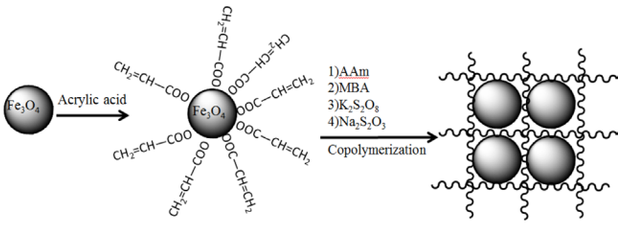

Fig. 1. Schematic representation for preparation of polymer-coated magnetite nanoparticle.

bent. Liu et al. [23] used this strategy to fabricate highly-controllable molecularly imprinting at super paramagnetic iron oxide nanoparticles. At the first step, grafting the acrylic acid via simple coordination reaction to magnetite nanoparticles surface results in formation of monolayer molecules with polymerizable vinyl end groups directed outward which helps polymerization to occur efficiently on the surface of nanoparticles. Subsequently, by addition of functional monomer (acrylamide) and cross-linking agent in the presence of initiator and accelerator, the cross-linked copolymer surrounded magnetic nanoparticles is synthesized. To complete polymerization, the beaker was kept in an oven at 45°C for about 1 h. The composition of monomer and cross-linker can influence the physicochemical properties of synthesized composite such as swelling and metal ion adsorption capacity. This will be discussed in detail in the following sections.

3.2. Characterization of Fe_3O_4 and Fe_3O_4/polymer

The morphology and size of Fe_3O_4/polymer nanoparticles in comparison with bare Fe_3O_4 were studied by SEM (Fig. 2). It seems that the synthesized MNPs have rather high surface area, and the substructures nearly are of spherical shaped nanocrystallites with dimensions less than 50 nm. The cross-linked copolymer homogenously covered the nanaparticles surface as evidenced by changing dendritic surface nanostrucures to more smoothed surface. The photograph of the Fe_3O_4/polymer nanocomposite hydrogel and cross-linked copolymer hydrogel are also provided in Fig. 2.

The crystallinity of both Fe_3O_4/polymer and pure magnetite nanoparticles was investigated by XRD. The results shown in Fig. 3A indicate that the iron oxide nanoparticles, which were prepared in the absence of copolymer, had six characteristic diffraction peaks at 2θ of 30.1, 35.4, 42.9, 52.7, 57.5 and 62.7, representing corresponding indices of (220), (311), (400), (422), (511) and (440), respectively, of iron oxide [33]. All peak positions were basically consistent with the standard data of the Fe_3O_4 structure (JCPDS 85-1436) and no other unexpected peaks were present. The hydrogel coated magnetic nanoparticles exhibited the same peaks as iron oxide nanoparticles with no observable shifts. This indicated that the Fe_3O_4/polymer composite particles have a highly crystalline cubic spinal structure confirming that crystalline structures of the magnetic nanoparticle did not change as they were surrounded by hydrogel shell.

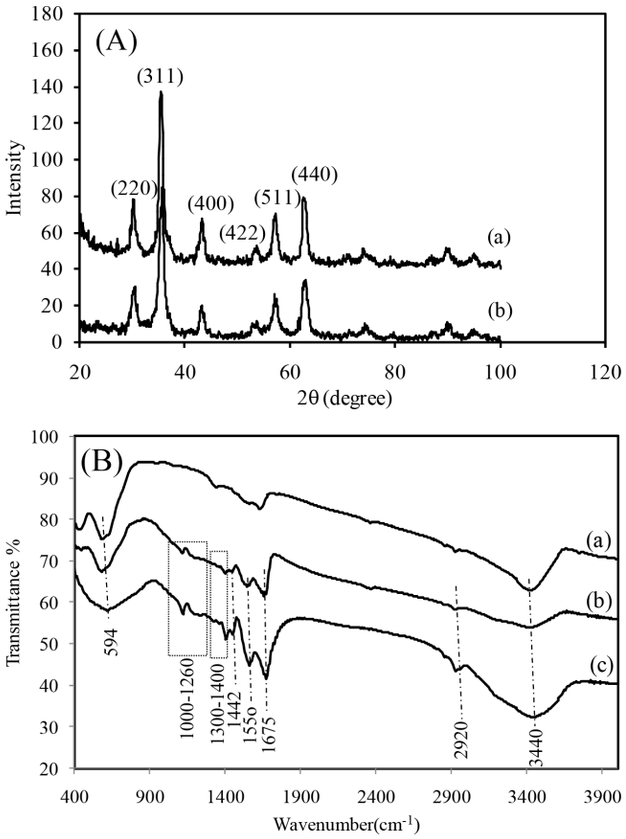

Fig. 3. (A) The X-ray diffraction results of the (a) magnetic nanoparticles, and (b) polymer-coated magnetic particles. (B) FTIR spectra of (a) magnetic nanoparticles, (b) polymer-coated magnetic nanoparticles and (c) dried polymer.

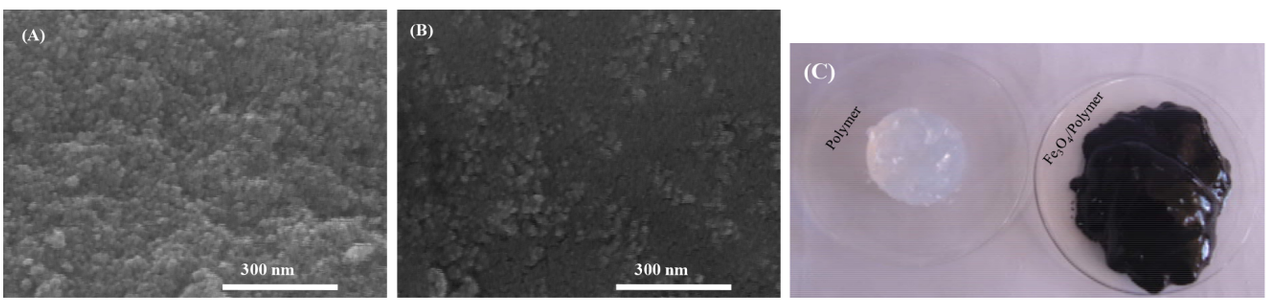

Fig. 2. SEM micrograph of pure (A), and polymer-coated (B), magnetite nanoparticles. (C) The digital camera photograph of polymer and polymer-coated magnetic nanoparticles as indicated.

A reliable method for following the variations in the functional groups is the FTIR technique. The FTIR spectra of Fe_3O_4, Fe_3O_4/polymer nanoparticles and the dried polymer are shown in Fig. 3B. The broad absorption band at 3440 cm^{-1} indicates the O–H stretching of residual water and surface hydroxyl groups [34]. In the spectra of both polymer and Fe_3O_4/polymer, a peak corresponds to (N–H) stretching of amide groups of hydrogel polymer is observable at 3210 cm^{-1}. The bands at low wavenumbers (594 cm^{-1}), for three samples, are related to vibration of the Fe–O bonds [31]. The peak observed around 2920 cm^{-1} in the spectra of both Fe_3O_4/polymer nanoparticles and the dried polymer is due to C–H stretching of polymer backbone. The $-CH_2$ groups on the chain show an absorption peak at 1442 cm^{-1}. The absorbance at 1675 cm^{-1} can be attributed to the C=O group of the acrylamide unit and the absorbance at 1550 cm^{-1} is assigned to the –COONa group. The characteristic peaks at 1300–1400 cm^{-1} are due to the presence of a C–N vibration, and the peak at 1000–1260 cm^{-1} is due to C–O. The above results revealed that the hydrogel coated the iron oxide nanoparticles successfully.

The TGA curves for the polymer-coated iron oxide nanoparticles, naked iron nanoparticles and copolymer are shown in Fig. 4A in order to determine the content of organic functional groups of each sample. The weight loss of pure Fe_3O_4 nanoparticles is around 10% at 600°C and is attributed to dehydration of the hydroxyl groups on the nanoparticles surface [33]. For copolymer and polymer-coated iron oxide nanoparticles, loss of residual water occurred in temperature range of 25–250°C. Decomposition of copolymer started at about 280°C and completed at 500°C. According to the TGA curves, the polymer content of Fe_3O_4/polymer nanoparticles was evaluated to be 39% by weight.

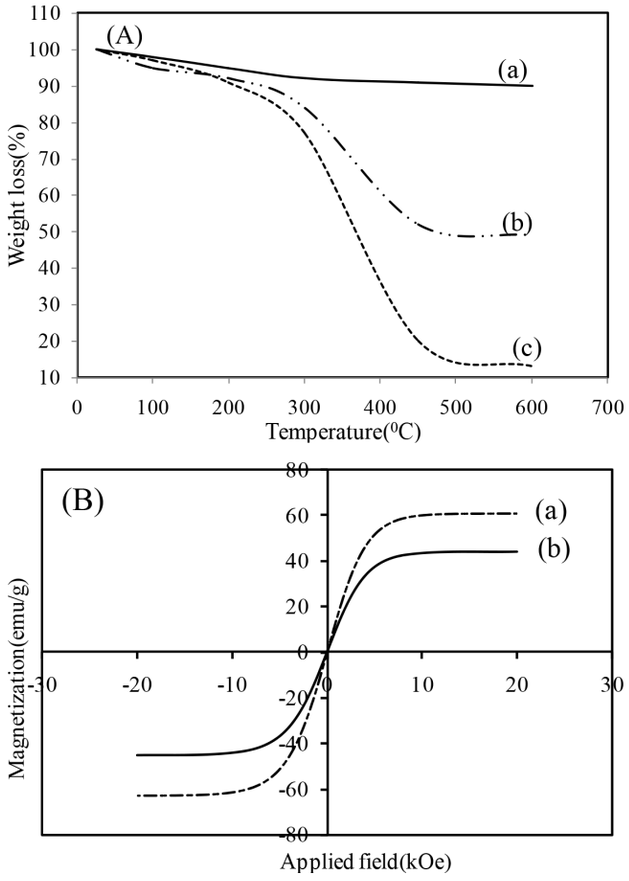

Fig. 4. (A) Thermogravimetric analysis of (a) Magnetic nanoparticles, (b) polymer-coated magnetic nanoparticles and (c) dried polymer. (B) Magnetization curve of (a) magnetic nanoparticles, (b) polymer-coated magnetic nanoparticles at room temperature.

The magnetic properties of the Fe_3O_4/polymer particles were also investigated on a vibrating sample magnetometer (VSM) system at room temperature (Fig. 4B). They showed super paramagnetic behavior at room temperature as indicated by the absence of remainance and coercivity upon removing an applied external magnetic field [34]. The saturation magnetizations (M_s) were obtained as 60.9 and 43.9 emu/g for naked Fe_3O_4 and Fe_3O_4/polymer nanocomposite, respectively. A 27.0% decrease in M_s as a consequence of modification with polymer can be explained by considering diamagnetic contribution of the thick polymer shell surrounding the magnetic cores [35]. The electron exchange between the ligand and the surface atoms could also quench the magnetic moment [36].

The pHpzc, i.e. the pH at which the net surface charge is zero, was determined by combined influence of all functional groups on the surface of polymer-coated magnetic nanoparticles. At pH < pHpzc, the surface has a net positive charge; while at pH > pHpzc, the surface has a net negative charge [37]. The pH_{pzc} values of Fe_3O_4 and Fe_3O_4/polymer were determined as 6.3 and 6.5, respectively. The data revealed that both adsorbents were positively charged at pHs lower than 6.5. Furthermore, Fe_3O_4/polymer shows buffering behavior in wider pH range compared with the unmodified Fe_3O_4 which is a consequence of functional groups of polymer shell and would be helpful in practical applications.

3.3. Metal ion uptake

A great deal of work has been done for investigating the interaction between metal ions and acrylic acid, poly(acrylic acid), poly(AAc-co-AAm) hydrogel as well as poly(acrylic acid) which modify solid supports such as magnetite nanoparticles [32,38,39]. The polymeric acid (which is a polyelectrolyte) can dissociate to H^+ and carboxyl anion, $-COO^-$, in an aqueous solution. When metal ions are added into polymeric acid solution, they can associate via electrostatic forces. The pH of the solution, the extent of carboxyl functional groups and the ratio of the residual functional groups to metal ions concentration can influence the metal ions adsorption mechanism and adsorption capacity. The efficiencies of the prepared Fe_3O_4 and Fe_3O_4/polymer as adsorbents for removal of Cd(II) and Zn(II) from aqueous solutions were investigated under different experimental conditions in order to find the optimum parameters. The effect of hydrogel composition, solution pH, contact time, metal ions concentrations and ionic strength will be discussed as below.

3.3.1. Effect of polymer composition

The effects of the content of the acrylic acid in the copolymer, and the content of the cross-linking agent on the adsorption performance were evaluated. As depicted in

Fig. 5A, Zn(II) removal efficiency sharply improved with increasing AAc monomer and reaches its maximum value when homopolymer of AAc was used. Since PAA is a polyelectrolyte and the affinity of carboxylic acid group for heavy metal ions is stronger than that of amide group, its metal removal capacity is considerably higher than that of copolymer containing AAm. The other reason may be sterical hindrance which prevents the interaction of the metal ion with the carboxylate functional groups in the copolymer. The Cd(II) adsorption efficiency although increases with increasing AAc percentage but the process is less sensitive when compared with Zn(II) adsorption which is in consistent with what was observed previously by other researchers [32]. Furthermore, the presence of less than 20% AAm ensures the maximum adsorption.

The effect of cross-linking agent on metal ion adsorption efficiency of the synthesized Fe_3O_4/polymer was examined by changing the cross-linking agent in the range of 0.3 to 5% (Fig. 5B). By increasing the percentage of cross-linking agent, the metal ion removal efficiency rapidly rises to its maximum value and then sharply decreases. An increase in the degree of cross-linking shortens the length of chain segments of copolymer network and increases the cross-linking density. Low content of MBA can ensure the formation of pores in copolymer to more efficient uptake of metal ion and water. But highly cross-linked copolymer has smaller pores, and shows lower flexibility which makes difficulties in the metal ion diffusion and interaction.

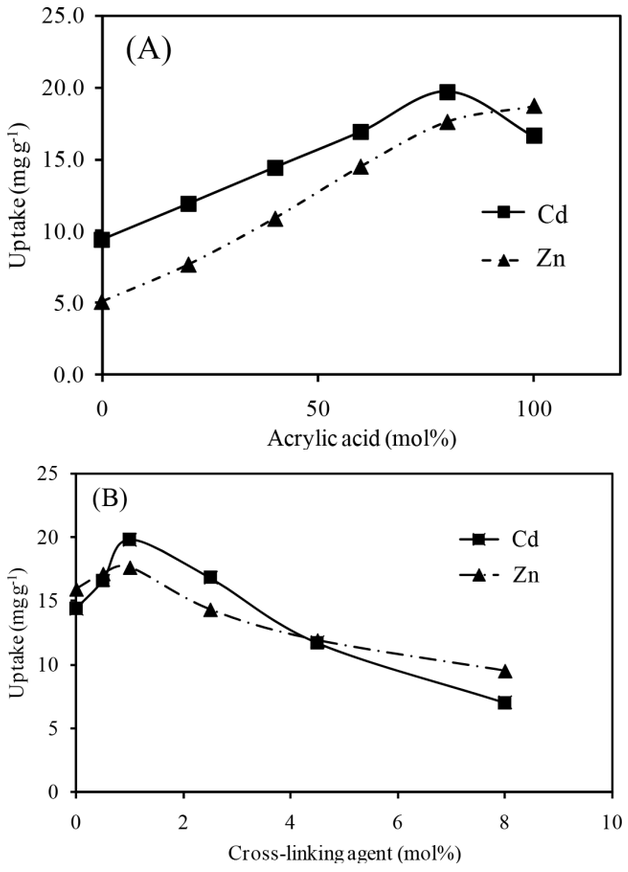

Fig. 5. (A) Uptake of metal ions on polymer- coated magnetic nanoparticles with different content of acrylic acid. (B) Uptake of metal ions on polymer-coated magnetic nanoparticles with different content of cross-linking agent.

3.3.2. Effect of pH

At different pH values, the protonation-deprotonation behaviors of acidic and basic groups would be influenced. The pH of solution can also affect adsorption because it determines the metal ion speciation in solution. The experimental results for the effects of pH on the non-competitive adsorption of metal ions are shown in Fig. 6A. The adsorption increased significantly with increasing pH (within pH 2.0–5.0). At low pH values, there is competition between metal ion and proton to interact with the carboxylate ion of the polymer [40].

By increasing pH to 8.0, the adsorption reaches its maximum value and then decreases slowly. As pointed out previously, pH has critical effect on the concentrations of metal ions, the charge of the metal species present in the solution and consequently on their affinity for being adsorbed. For

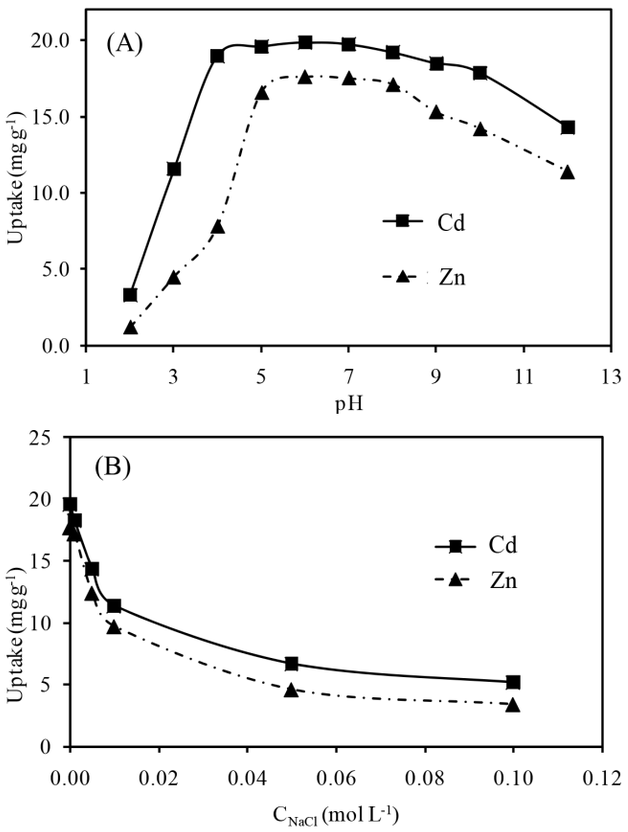

Fig. 6. (A) Effect of initial pH solution on uptake of metal ions from aqueous solutions using polymer-coated magnetic nanoparticles; parameters: initial metal concentration of 20 mg L^{-1}; pH 6.0; adsorbent mass of 10 mg; contact time of 5 min; temperature at 25°C. (B) Influence of electrolyte on the uptake of metal ions on polymer- coated magnetic nanoparticles. Adsorption conditions are the same as (A).

instance, at pH ≤ 8.0, M(II) is mainly found as M^{2+} and from this value to higher pH, M(II) presents as chemical forms of $M(OH)_2$, $M(OH)^+$, $M(OH)_3^-$ and $M(OH)_4^{2-}$ [41]. At higher pH values, the small decrease in the uptake capacity was likely due to the formation of soluble hydroxylated complexes of the metal ions as well as metal hydroxide precipitate and their lower affinity toward the active adsorption sites. The pH of 6.0 was selected as the optimum value for further investigation. This value was not only near the initial pH of the adsorbent but also ensured the highest adsorption efficiency through ruling out the competition effect of H^+ with metal ion. Moreover, the M^{2+} ion would be the predominant species in this condition.

3.3.3. Effect of solution ionic strength

It was found that the binding capacities decreased with increasing the NaCl concentration from 0.001 to 0.1 mol/L. Fig. 6B shows the amount of metal ion adsorbed as affected by different concentrations of the background electrolyte. The slower decrease in Cd(II) adsorption, compared with Zn(II), confirmed that the binding was more electrostatic in nature for the later. These results indicated that ionic strength might influenced the adsorption capacity of the adsorbent. This could be attributed in part to the competition between M^{2+} and Na^+ ions for the surface sites as the ionic strength increased. The binding capacities, even at these high ionic strengths, were sufficient for the composite to bind Zn(II) and Cd(II) from natural waters.

3.3.4. Effect of nanoparticle dosage

The effect of adsorbent dosage on non-competitive removal of each metal ion was investigated by dispersing different amounts of adsorbent (2.0–25.0 mg) in separate beakers containing fixed amount of metal ions (20.0 mg L^{-1}) for a 5 min contact time. It was observed that with the increase in adsorbent dose from 2.0 to 10.0, the adsorbed amount of metal ions increased from 4.9 and 4.8 mg/g to 19.7 and 17.6 mg/g for Cd(II) and Zn(II), respectively, (Fig. 7A). This can be explained by considering the fact that at a higher adsorbent dosage, extra adsorption sites are available for metal ion binding. Further increase in the adsorbent dosage resulted in more efficient removal of Zn(II), but did not significantly affect the removal efficiency of Cd(II). Hence, the optimum dosage of Fe_3O_4/polymer powder, for non-competitive removing of both metal ions from their individual solutions, was found to be 10 mg.

3.3.5. Effect of contact time

Time course of the metal ions adsorption by Fe_3O_4/polymer composite was investigated from 1 up to 30 min to determine the time at which equilibrium adsorption took place. It is shown in Fig. 7B that the adsorption equilibrium was achieved to a level of about 83% within 3 min for both metal ions. The absorption increased up to 5 min and then leveled off. Therefore, an adsorption time of 5 min was selected throughout the experiments. The high surface area of Fe_3O_4/polymer, homogeneous distribution of the nanosorbents throughout the sample and absence of internal diffusion resistance could be the possible reasons for achieving such a fast extraction process.

3.3.6. Effect of metal ion concentration

Another important variable that can affect the adsorption process and is crucial in practical application of adsorbent is the metal ion concentration. This will determine the concentration range of the metal ion at which its quantitative removal can be performed with high efficiency. To illustrate this, different initial concentrations (in the range of 1–300 mg/L) of Cd(II) and Zn(II) were adsorbed by Fe_3O_4/polymer under the previously determined optimum experimental conditions. Fig. 8A demonstrates adsorption efficiency vs. initial molar concentrations of the metal

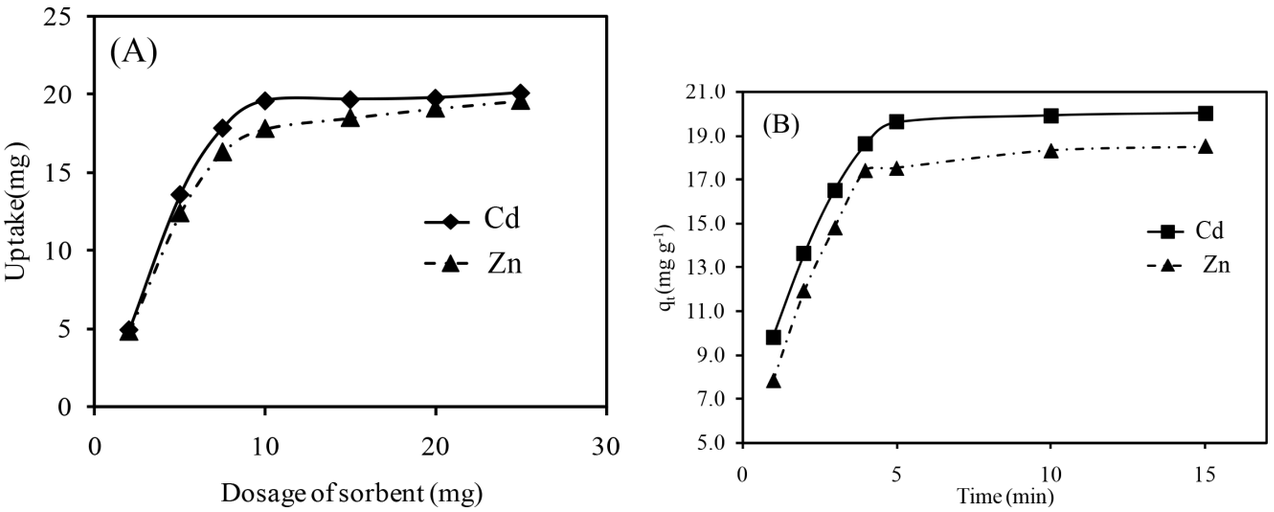

Fig. 7. (A) Effect of initial dosage of polymer-coated magnetic nanoparticles on uptake of metal ions. Experimental conditions: pH 6.0, initial metal concentration of 20 mg L^{-1}; contact time of 5 min; temperature at 25°C. (B) Effect of stirring time on uptake of metal ions. Experimental conditions: adsorbent mass of 10 mg, pH 6.0, initial metal concentration of 20 mg L^{-1}; temperature at 25°C.

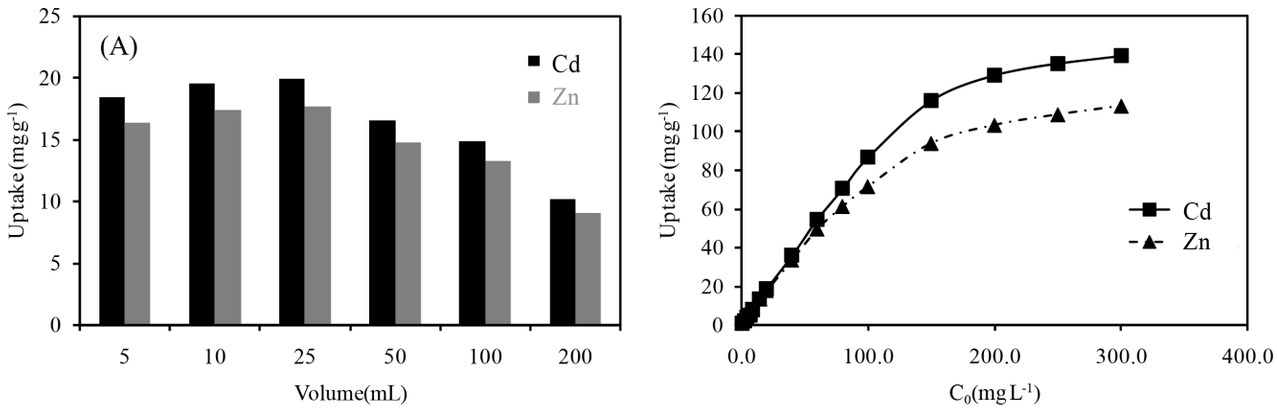

Fig. 8 (A) Effect of initial metal ion concentration on the uptake of metal ions. Experimental conditions: adsorbent mass of 10 mg, pH 6.0; contact time of 5 min; temperature at 25°C. (B) Effect of sample volume on adsorption of metal ions.

ions in a non-competitive way. It seems that Fe_3O_4/polymer nanoparticles have greater efficiency for removal (in gram) of both Cd(II) than Zn(II) but it reveals that the Zn(II) removal capacity (in mole) is higher than Cd(II).

3.3.7. Effect of sample volume

The efficiency of Fe_3O_4/polymer for uptaking the metal ions from different sample volumes was tested by adsorption of a fixed amount of individual metal ions in sample volumes from 5.0 to 200.0 mL under optimized conditions. As shown in Fig. 8B, the adsorption efficiency shows a maximum at 25 mL for both metal ions. At 200 mL, the adsorption decreases to 50% of the corresponding values at 25 mL. The decrease can be simply explained by considering the fact that in higher volumes the probability of contact between adsorbate and adsorbent is lowered. The small decrease in adsorption capacity at low volumes could be due to insufficient dispersion of sorbent which causes high hydrogen binding between functional groups or induced aggregation in the presence of metal ion. This reduced the surface sites of adsorbent to bind with metal ions in solution.

3.4. Adsorption kinetics, isotherms and thermodynamics

3.4.1. Adsorption kinetic modeling

Application of the adsorption techniques to larger scale processes requires explanation of the kinetic parameters and adsorption characteristics of the adsorbent materials [42]. In order to investigate the mechanism of adsorption, particularly the potential rate-determining step, the time course data were fitted to linearized forms of pseudo-first-order and pseudo-second-order models [43,44]. Suitability of both models was evaluated by comparing correlation coefficients (R^2). The kinetic parameters calculated using linear regression analysis along with correlation coefficients are illustrated in Table 1. For both metal ions, the second-order model has correlation coefficients more closer to 1 and the q_e values obtained from the plots ($q_{e,theory}$) are almost similar to the experimental values ($q_{e,exp}$). Generally, the mechanism of adsorption into hydrogels depends on the macromolecular relaxation of the tree-dimensional polymer network [45]. However, it has been frequently reported that the adsorption kinetics of metal ions onto polymer-coated nanoparticles were matched with pseudo-first-order and pseudo-second-order models [46,47]. This could be attributed to the small size of particles, thin polymer coting layer, lower crosslinking degree and low rigidity of polymer backbone. The results showed better fitness of the experimental data to pseudo-second-order kinetic model suggesting that chemisorption may be the rate-limiting step that controls the adsorption process and that mass transfer in solution and inner particle diffusion are not involved [48].

3.4.2. Adsorption isotherm modeling

The details of metal ion adsorption process by Fe_3O_4/polymer can be clarified by evaluation of adsorption isotherms. This can be obtained by fitting the experimental data to the linear forms of the two most common adsorption models, known as Freundlich and Langmuir adsorption isotherm models [49]. The plots are shown in Fig. 9

Table 1
Calculated kinetic parameters for pseudo first-order, and second-order kinetic models, for Cd(II) and Zn(II) adsorption using Fe_3O_4/polymer as the adsorbent

Metal ion	Pseudo first-order model				Pseudo second-order model			
	$q_{e,exp}$ (mg g^{-1})	k_1 (min^{-1})	$q_{e,cal}$ (mg g^{-1})	R^2	$q_{e,exp}$ (mg g^{-1})	k_2 (min^{-1})	$q_{e,cal}$ (mg g^{-1})	R^2
Zn(II)	18.6	0.396	12.58	0.956	18.6	0.033	19.3	0.993
Cd(II)	19.4	0.347	10.7	0.842	19.4	0.058	19.9	0.992

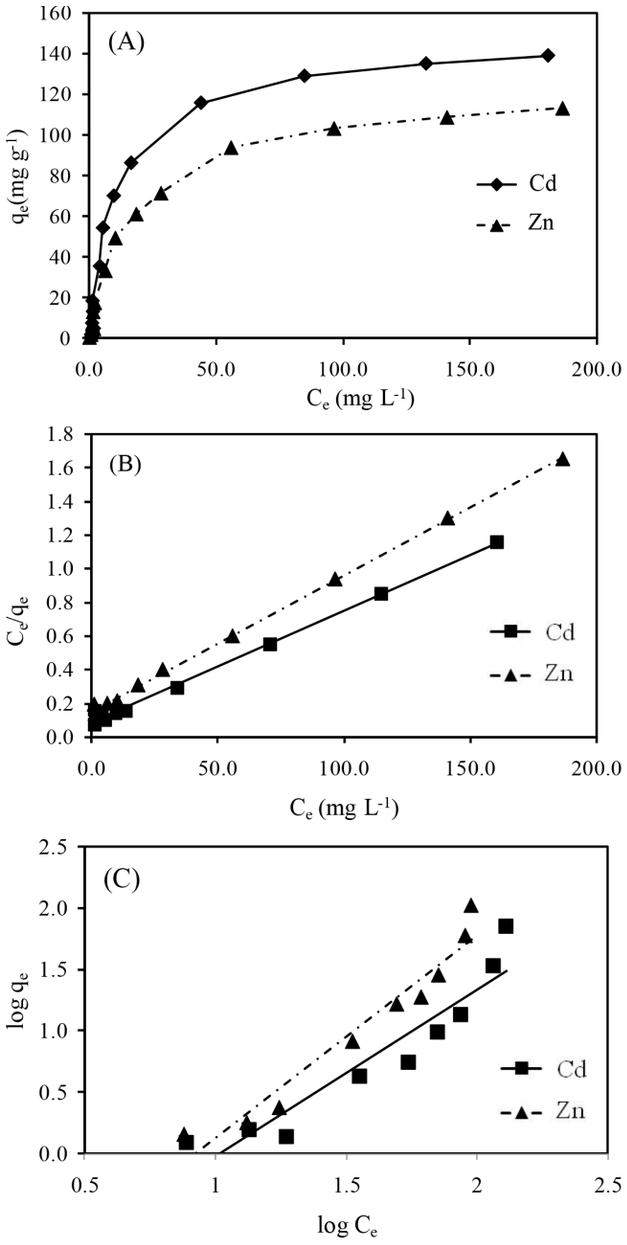

Fig. 9. (A) Equilibrium isotherms plots; (B) Langmuir adsorption isotherm, and (C) Freundlich adsorption isotherm.

and the corresponding calculated parameters along with correlation coefficients are summarized in Table 2. Considering correlation coefficient as criteria for comparison, the Langmuir model could better explain the adsorption results of both metal ions. This indicates to the adsorbed monolayer coverage of metal ions on the adsorbent surface; as Langmuir model says, all adsorption sites are equal with uniform adsorption energies without any interaction between the adsorbed species. It could be reasonable, because metal ions bind to carboxylate functional groups and has no tendency to bind with additional metal ions. The R_L values obtained as 2.4×10^{-4} and 2.8×10^{-4} for Cd(II) and Zn(II), respectively, confirm the suitability of the adsorbent for metal ion removal. Maximum adsorption capacity (q_{max}) obtained as 142.8 and 111.1 mg/g for Cd(II) and Zn(II), respectively, are higher than most other previously reports on metal ion removal on nanoadsorbents as will be discussed in the following sections.

3.4.3. Thermodynamics of adsorption

Thermodynamic parameters, including Gibbs free energy change (ΔG), enthalpy change (ΔH) and entropy change (ΔS) are defined to evaluate whether the adsorption process takes place spontaneously. The calculated parameters are summarized in Table 3. The negative values of free energy change indicate the spontaneous nature of sorption and confirms affinity of sorbents for the metal ions. On the other hand, the positive value of ΔH suggests an endothermic nature of the adsorption process. The positive values of ΔS are the consequence of metal ion desolvation during the adsorption process. The higher values of |TΔS| relative to |ΔH| indicates that the adsorption process is entropically driven.

3.5. Desorption and reusability studies

Regeneration is a very important factor which determine the suitability of adsorbents for practical applications such as water purification and industrial wastewater treatments, because it can significantly affects the cost and time of pollutant removal [50]. Due to reversible adsorption process, the regeneration of the adsorbent is possible. Therefore, to investigate the reusability of the magnetic Fe_3O_4/polymer composite, cyclic adsorption/desorption study was carried out for the metal ions. As mentioned in the previous sections, adsorption efficiency significantly reduced as ionic strength increased and pH decreased. This observation provided the clue to select 0.01 M HCl as the eluent for desorption of metal ions. It was notable that desorption equilibrium was achieved within 10 min which is considerably lower than that of most similar researches (Section 3.8). This could be due to the absence of internal diffusion resistance [43]. The recovered hydrogel was reused five times with less than 5% reduction recovery percentages (Fig. 10).

Table 2
Isotherm constants and regression data of various adsorption isotherms for adsorption of Cd(II) and Zn(II) on Fe_3O_4/polymer.

Metal ion	Langmuir				Freundlich		
	q_{max} (mg g^{-1})	k_L (L g^{-1})	R^2	R_L	$1/n$	k_F (L g^{-1})	R^2
Zn(II)	111.1	13.88	0.999	2.4×10^{-4}	1.65	0.30	0.943
Cd(II)	142.8	11.85	0.997	2.8×10^{-4}	1.46	0.032	0.857

Table 3
Thermodynamic parameters of adsorption of Zn(II), Cd(II) on Fe_3O_4/polymer

Metal ion	ΔS (J mol^{-1} K^{-1})	ΔH (kJ mol^{-1})	ΔG (kJ mol^{-1})			
			293	303	313	323
Cd(II)	30.578	3.846	−5.111	−5.416	−5.722	−6.028
Zn(II)	34.261	5.643	−4.394	−4.737	−5.079	−5.422

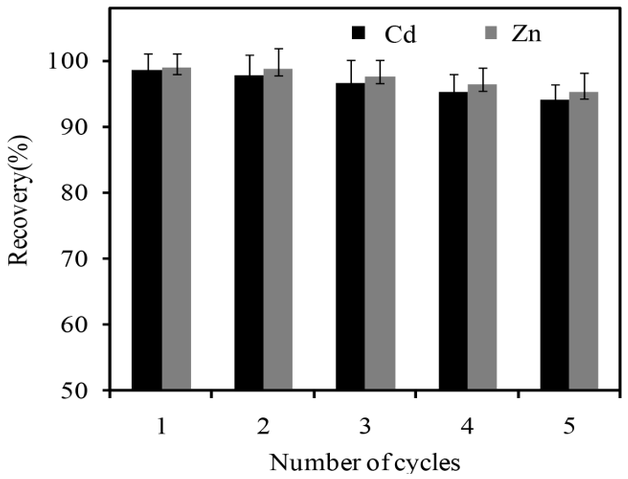

Fig. 10. Metal ion recoveries calculated for five consecutive adsorption-desorption cycles. Initial metal concentration of 40 mg L^{-1}; adsorbent mass of 10 mg; adsorption time of 5 min; desorption time 10 min; temperature at 25°C.

The possibility of reusing the reactive polymer for several times makes it economically suitable for application purposes. Furthermore, good recoveries even after five cycles are promising to be useful in preconcentration and recycling purposes.

3.6. Competitive adsorption

Effect of other heavy metal ions on adsorption of Cd(II) and Zn(II) was investigated by acquiring removal efficiency for metal ions, individually or in binary mixtures containing equal quantities (20 mg/L) of metal ions. It was observed that the order of removal efficiencies in mmol/g for metal ions was Cu(II) > Zn(II) > Cd(II) > Pb(II) > Hg(II), implying the stronger affinity of the adsorbent for metal ions in the mentioned order. The observation could be explained by hard-soft interaction when the hard carboxylate group of polymer interacts better with harder metal ions. For binary mixtures, the removal efficiency for Cd(II) and Zn(II) decreased significantly in the presence of Cu(II), while Hg(II) had the least effect on the removal efficiencies of Cd(II) and Zn(II).

3.7. Application

The performance of the Fe_3O_4/polymer as metal ions adsorbent was evaluated by spiking Zn(II) or Cd(II), in freshly collected tap water and mineral water samples. The results in Table 4 indicate that ionic strength causes less adsorption efficiency; the removal efficiency was much better in mineral samples compared to tap water samples. These results imply the good performance of the adsorbent for removing these metal ions from real water samples.

3.8. Comparison of Zn(II) and Cd(II) removal with different magnetic nanoadsorbents reported in literature

Important parameters such as maximum adsorption capacity, adsorption time, and desorption time were compared to other magnetic nanoadsorbents and the results are summarized in Table 5. The adsorption capacities of Fe_3O_4/polymer toward both metal ions were higher than that of most adsorbents [50–52,55,57,60–64]. One of the most important parameters in designing and commercialization of adsorbents for removal of pollutants from waste waters is adsorption/desorption time which is quite shorter for the produced adsorbent compared with other previously reported ones [51–59,61–64].

Table 4
The adsorbent performance for removal of spiked metal ions from Tap water* and mineral water** samples.

Water sample	Added (mg L^{-1})		Removal (mg L^{-1})	
	Cd(II)	Zn (II)	Cd(II)	Zn (II)
Mineral water	20.0	20.0	18.7 (± 0.8)***	17.8 (± 0.8)
	40.0	40.0	37.2 (± 1.3)	35.1 (± 1.2)
Tap water	20.0	20.0	17.6 (± 0.6)	15.9 (± 0.7)
	40.0	40.0	36.1 (± 1.1)	32.7 (± 1.2)

*The parameters of tap water determined by the reference lab: EC = 975, TDS = 643, Total Hardness = 450, pH = 7.2, Cl^- = 2.5, Ca^{2+} = 5.0, Mg^{2+} = 4.0, Na^+ = 0.84.
**The parameters of mineral water labeled by the company: EC = 294, TDS =185, Total Hardness =132, pH = 7.5, Cl^- = 3.7, Ca^{2+} = 48, Mg^{2+} = 8, Na^+ = 2.
***The values in parentheses show SD for three replicate analyses.

Table 5
Magnetic adsorbents reported in literature for Cd(II) and Zn(II) adsorption

Adsorbent	q_{max} (mg/g)		Adsorption/desorption time		[Ref.]
	Cd(II)	Zn(II)	Cd(II)	Zn(II)	
Magnetic chitosan-based hydrogels	135.5	–	24 h/ 24 h	–	[50]
4-Phenyl-3-thiosemicarbazide modified magnetic nanoparticles	125.0	57.8	15 min/3 h	15 min/3h	[51]
Magnetic hydrogels	140.8	–	12 h/24 h	–	[52]
Magnetic chelating resin with iminodiacetate functionality	259.6	127.2	3 h/3 h	–	[53]
Magnetic hydroxyapatite nanoparticles	220.8	140.6	24 h/ 24 h	24 h/ 24 h	[54]
Magnetic graphene oxide sheets	13.4	–	24 h/–	–	[55]
∝-Ketoglutaric acid-modified magnetic chitosan	201.2	–	90 min/2 h	–	[56]
Fe_3O_4/cyclodextrin polymer nanocomposites	27.7	–	45 min/ 2 h	–	[57]
Amine-functionalized mesoporous Fe_3O_4 nanoparticles	523.6	–	2 h/–	–	[58]
Thiourea-modified magnetic ion-imprinted chitosan/TiO_2	256.4	–	6 h/6 h	–	[59]
Sodium dodecyl sulphate coated magnetite nanoparticles	–	59.2	–	1 min/5 min	[60]
Amino-functionalized Fe_3O_4@SiO_2 magnetic nanomaterial	22.5	–	24 h/12 h	–	[61]
Dendrimer-conjugated magnetic nanoparticles	–	24.3	1 h/30 min	–	[62]
Magnetic manganese dioxide	31.5	–	10 min/–	–	[63]
Magnetic hydrogels	83.3	–	12 h/12 h	–	[64]
Fe_3O_4/polymer nanocopmosite	142.8	111.1	5 min/10min	5 min/10 min	This work

4. Conclusions

In the present study, copolymerization of acrylic acid and acrylamide was done in the presence of Fe_3O_4 nanoparticles for fabrication of superparamagnetic Fe_3O_4/polymer nanocomposites, which showed great promise in removal of Zn (II) and Cd(II) from aqueous media. The prepared magnetic nanoparticles can be well dispersed in the aqueous solutions. It was found that the adsorption equilibrium was achieved in 5 min and the adsorption efficiency depended on pH and reached to its maximum in the pH range of 5.0–8.0. Pseudo-second-order kinetic model was properly fitted to the experimental data. The Langmuir model was successfully used to determine adsorption isotherms confirming a monolayer adsorption with maximum adsorption capacities of 142.8 and 111.1 mg/g for Cd(II) and Zn(II), respectively. Thermodynamic studies demonstrated that the Gibbs free energy was negative and the adsorption process was spontaneous. Adsorbed metal ions can be easily recovered and adsorbent can be regenerated and reused at least for five times without any significant (less than 5%) losing in its adsorption capacity.

Acknowledgments

The authors wish to acknowledge the support of this work by Shiraz University Research Council.

References

[1] B. Bergbäck, K. Johansson, U. Mohlander, Urban metal flows–a case study of Stockholm. Review and conclusions, Water, Air Soil Pollut. Focus, 1 (2001) 3–24.
[2] M. Winter, R.J. Brodd, What are batteries, fuel cells, and supercapacitors? Chem. Rev., 104 (2004) 4245–4270.
[3] R.M. de Souza, A.L.S. Meliande, C.L.P. da Silveira, R.Q. Aucélio, Determination of Mo, Zn, Cd, Ti, Ni, V, Fe, Mn, Cr and Co in crude oil using inductively coupled plasma optical emission spectrometry and sample introduction as detergentless microemulsions, Microchem. J., 82 (2006) 137–141.
[4] G. Schwartz, I.M. Reis, Is cadmium a cause of human pancreatic cancer?, Cancer Epidemiol. Biomark. Preven., 9 (2000) 139–145.
[5] M.M.S. Saif, N.S. Kumar, M.N.V. Prasad, Binding of cadmium to strychnos potatorum seed proteins in aqueous solution: adsorption kinetics and relevance to water purification, Colloids Surf., B 94 (2012) 73–79.
[6] L. Friberg, C.G. Elinder, Encyclopedia of Occupational Health, 3rd ed.,, Geneva, International Labor Organization, 1985.
[7] Q. Tang, X. Tang, M. Hu, Z. Li, Y. Chen, P. Lou, Removal of Cd(II) from aqueous solution with activated Firmiana simplex leaf: Behaviors and affecting factors, J. Hazard. Mater., 179 (2010) 95–103.
[8] WHO, Guidelines for Drinking-Water Quality, 4th ed., World Health Organization, Geneva, Switzerland 2011.
[9] N.M. Mubarak, R.F. Alicia, E.C. Abdullah, J.N. Sahu, A.B.A. Haslija, J. Tan, Statistical optimization and kinetic studies on removal of Zn(II) using functionalized carbon nanotubes and magnetic biochar, J. Environ. Chem. Eng., 1 (2013) 486–495.
[10] T.A. Kurniawan, G.Y.S. Chan, W.H. Lo, S. Babel, Physico-chemical treatment techniques for wastewater laded with heavy metals, Chem. Eng. J., 118 (2006) 83–98.
[11] S. Babel, T.A. Kurniawan, Low-cost adsorbents for heavy metals uptake from contaminated water: a review, J. Hazard. Mater., 97 (2003) 219–243.
[12] S.T. Ramesh, N. Rameshbabu, R. Gandhimathi, P.V. Nidheesh, M.S. Kumar, Kinetics and equilibrium studies for the removal of heavy metals in both single and binary systems using hydroxyapatite, Appl. Water Sci., 2 (2012) 187–197.
[13] J. Kour, P.L. Homagai, M.R. Pokherel, K.N. Ghimire, Kush - A Potential Biosorbent in the removal of Cd (II) and Zn (II) from aqueous solution, J. Nepal Chem. Soc., 27 (2011) 107–114.

[14] F. Wu, Y.X. Zhang, Y.L. Chen, H. Qian, Recycle of Ag^{+} and Zn^{2+} with magnetic adsorbent in process of Its purification from wastewater, Clean – Soil, Air, Water, 42 (2014) 71–80.
[15] J.P. Ruparelia, S.P. Duttagupta, A.K. Chatterjee, S. Mukherji, Potential of carbon nanomaterials for removal of heavy metals from water, Desalination 232 (2008) 145–156.
[16] A.K. Mishra, A.K. Sharma, Synthesis of β-cyclodextrin/chitosan composites for the efficient removal of Cd(II) from aqueous solution, Int. J. Biol. Macromol., 49 (2011) 504– 512.
[17] R. Moreno-Tovar, E. Terrés, J. Rene Rangel-Mendez, Oxidation and EDX elemental mapping characterization of an ordered mesoporous carbon: Pb(II) and Cd(II) removal, Appl. Surf. Sci. 303 (2014) 373–380,
[18] J.H. Deng, X.R. Zhang, G.M. Zeng , J.L. Gong , Q.Y. Niu, J. Liang, Simultaneous removal of Cd(II) and ionic dyes from aqueous solution using magnetic graphene oxide nanocomposite as an adsorbent, Chem. Eng. J., 226 (2013) 189–200.
[19] M. Kumar, B.P. Tripathi, V.K. Shahi, Cross-linked chitosan/polyvinyl alcohol blend beads for removal and recovery of Cd (II) from wastewater, J. Hazard. Mater., 172 (2009) 1041–1048.
[20] T. Ahmad, H. Bae, I. Rhee, Y. Chang, J. Lee, S. Hong, Particle size dependence of relaxivity for silica-coated iron oxide nanoparticles, Curr. Appl. Phys., 12 (2012) 969–974.
[21] M.H. Liao, D.H. Chen, Preparation and characterization of a novel magnetic nano-adsorbent, J. Mater. Chem., 12 (2002) 3654–3659.
[22] C. Schweiger, C. Pietzonka, J. Heverhagen, T. Kissel, Novel magnetic iron oxide nanoparticles coated with poly(ethylene imine)-g-poly(ethylene glycol) for biomedical application: Synthesis, stability, cytotoxicity and MR imaging, Int. J. Pharm., 408 (2011) 130–137.
[23] B. Liu, M. Han, G. Guan, S. Wang, R. Liu, Z. Zhang, Highly-controllable molecular imprinting at superparamagnetic iron oxide nanoparticles for ultrafast enrichment and separation, J. Phys. Chem., C 115 (2011) 17320–17327.
[24] H. Bagheri, O. Zandi, A. Aghakhani, Extraction of fluoxetine from aquatic and urine samples using sodium dodecyl sulfate-coated iron oxide magnetic nanoparticles followed by spectrofluorimetric determination, Anal. Chim. Acta., 716 (2012) 61– 65.
[25] F. Jiang, Y. Fu, Y. Zhu, Z.K. Tang, P. Sheng, Fabrication of iron oxide/silica core–shell nanoparticles and their magnetic characteristics, J. Alloys Compd., 543 (2012) 43–48.
[26] M. Bonini, A. Wiedenmann, P. Baglioni, Synthesis and characterization of magnetic nanoparticles coated with a uniform silica shell, Mater. Sci. Eng., C 26 (2006) 745–750.
[27] L. Tonghuan, D. Guojian, D. Xiaojiang, W. Wangsuo, Y. Ying, Adsorptive features of polyacrylic acid hydrogel for UO_2^{2+}, J. Radioanal. Nucl. Chem., 297 (2013) 119–125.
[28] A. Khan, Preparation and characterization of magnetic nanoparticles embedded in microgels, Mate. Lett., 62 (2008) 898–902.
[29] J. Guo, X. Ye, W. Liu, Q. Wu, H. Shen, K. Shu, Preparation and characterization of poly(acrylonitrile-co-acrylic acid) nanofibrous composites with Fe_3O_4 magnetic nanoparticles, Mater. Lett., 63 (2009) 1326–1328.
[30] A.R. Mahdavian, M. Mirrahimi, Efficient separation of heavy metal cations by anchoring polyacrylic acid on superparamagnetic magnetite nanoparticles through surface modification, Chem. Eng. J., 159 (2010) 264–271.
[31] G. Absalan, M. Asadi, S. Kamran, L. Sheikhian, D.M. Goltz, Removal of reactive red-120 and 4-(2-pyridylazo) resorcinol from aqueous samples by Fe_3O_4 magnetic nanoparticles using ionic liquid as modifier, J. Hazard. Mater., 192 (2011) 476–484.
[32] Y. Zhang, Preparation of copolymers of acrylic acid and acrylamide for copper(II) capture from aqueous solutions, Master thesis, University of Waterloo, Canada 2009.
[33] D. Serrano-Ruiz, S. Rangou, A. Avgeropoulos, N.E. Zafeiropoulos, E. López–Cabarcos, J. Rubio-Retama, Synthesis and chemical modification of magnetic nanoparticles covalently bound to polystyrene-$SiCl_2$-poly (2-vinylpyridine), J. Polym. Sci., Part B: Polym. Phys., 48 (2010) 1668–1675.
[34] W.D. Callister, D.G. Rethwisch, Fundamentals of materials science and engineering: an integrated approach, John Wiley & Sons 2012.
[35] M. Rutnakornpituk, N. Puangsin, P. Theamdee, B. Rutnakornpituk, U. Wichai, Poly (acrylic acid)-grafted magnetic nanoparticle for conjugation with folic acid, Polymer 52 (2011) 987–995.
[36] M.H. Liao, D.H. Chen, Preparation and characterization of a novel magnetic nano-adsorbent, J. Mater. Chem., 12 (2002) 3654–3659.
[37] J. Park, J.R. Regalbuto, A simple, accurate determination of oxide PZC and the strong buffering effect of oxide surfaces at incipient wetness, J. Colloid Interface Sci., 175 (1995) 239–252.
[38] M.Y. Abdelaal, M.S. Makki, T.R. Sobahi, Modification and characterization of polyacrylic acid for metal ion recovery, Am. J. Polymer Sci., 2 (2012) 73–78.
[39] O. Moscoso-Londoño, J. Gonzalez, D. Muraca, C. Hoppe, V. Alvarez, A. López-Quintela, L. Socolovsky, K. Pirota, Structural and magnetic behavior of ferrogels obtained by freezing thawing of polyvinyl alcohol/poly (acrylic acid) (PAA)-coated iron oxide nanoparticles, Eur. Polymer J., 49 (2013) 279–289.
[40] D. Xu, X. Tan, C. Chen, X. Wang, Removal of Pb(II) from aqueous solution by oxidized multiwalled carbon nanotubes, J. Hazard. Mater., 154 (2008) 407–416.
[41] X.J. Hu, Y.G. Liu, G.m. Zeng, H. Wang, X. Hu, A.W. Chen, Y.Q. Wang, Y.M. Guo, T.T. Li, L. Zhou, Effect of aniline on cadmium adsorption by sulfanilic acid-grafted magnetic graphene oxide sheets, J. Colloid Interface Sci., 426 (2014) 213–220.
[42] J. He, Y. Lu, G. Luo, Ca(II) imprinted chitosan microspheres: An effective and green adsorbent for the removal of Cu(II), Cd(II) and Pb(II) from aqueous solutions, Chem. Eng. J., 244 (2014) 202–208.
[43] H. Wang, X. Yuan, Y. Wu, H. Huang, G. Zeng, Y. Liu, X. Wang, N. Lin, Y. Qi, Adsorption characteristics and behaviors of graphene oxide for Zn(II) removal from aqueous solution, Appl. Surf. Sci., 279 (2013) 432–440.
[44] Y.S. Ho, Review of second-order models for adsorption systems, J. Hazard. Mater., 136 (2006) 681–689.
[45] A.T. Paulino, L.A. Belfiore, L.T. Kubota, E.C. Muniz, E. B. Tambourgi, Efficiency of hydrogels based on natural polysaccharides in the removal of Cd^{2+} ions from aqueous solutions, Chem. Eng. J., 168 (2011) 68–76.
[46] A.Z.M. Badruddoza, Z.B.Z. Shawon, T.W.J. Daniel, K. Hidajat, M. Shahab-Uddin Fe_3O_4/cyclodextrin polymer nanocomposites for selective heavy metals removal from industrial wastewater, Selective adsorption of Pb(II), Cd(II), and Ni(II) ions from aqueous solution using chitosan–MAA nanoparticles, Carbohydr. Polym., 91 (2013) 322–332.
[47] A. Heidari, H. Younesi, Z. Mehraban, H. Heikkinen, Selective adsorption of Pb (II), Cd (II), and Ni (II) ions from aqueous solution using chitosan–MAA nanoparticles, Int. J. Biol. Macromol., 61 (2013) 251–263.
[48] Y.S. Ho, Adsorption of Heavy Metals from Waste Streams by Peat, Ph.D. Thesis, University of Birmingham, Birmingham, UK, 1995.
[49] D.D. Do, Adsorption analysis: Equilibria and kinetics, Imperial College Press, Daners, Massachusetts, USA 1998.
[50] A.T. Paulino, L.A. Belfiore, L.T. Kubota, E.C. Muniz, V.C. Almeida, E.B. Tambourgi, Effect of magnetite on the adsorption behavior of Pb(II), Cd(II), and Cu(II) in chitosan-based hydrogels, Desalination, 275 (2011) 187–196.
[51] K. Zargoosh, H. Zilouei, M.R. Mohammadi, H. Abedini, 4-Phenyl-3-thiosemicarbazide modified magnetic nanoparticles: synthesis, characterization and application for heavy metal removal, CLEAN–Soil, Air, Water, 42 (2014) 1208–1215.
[52] O. Ozay, S. Ekici, Y. Baran, N. Aktas, N. Sahiner, Removal of toxic metal ions with magnetic hydrogels, Water Res., 43 (2009) 4403–4411.
[53] C.Y. Chen, C.L. Chiang, P.C. Huang, Adsorptions of heavy metal ions by a magnetic chelating resin containing hydroxy and iminodiacetate groups, Sep. Purif. Technol., 50 (2006) 15–21.

[54] Y. Feng, J.L. Gong, G.M. Zeng, Q.Y. Niu, H.Y. Zhang, C.G. Niu, J.H. Deng, M. Yan, Adsorption of Cd (II) and Zn (II) from aqueous solutions using magnetic hydroxyapatite nanoparticles as adsorbents, Chem. Eng. J., 162 (2010) 487–494.
[55] X.J. Hu, Y.G. Liu, G.M. Zeng, H. Wang, X. Hu, A.W. Chen, Y.Q. Wang, Y.G. Guo, T.T. Li, L. Zhou, Effect of aniline on cadmium adsorption by sulfanilic acid-grafted magnetic graphene oxide sheets, J. Colloid Interface Sci., 426 (2014) 213–220.
[56] G. Yang, L. Tang, X. Lei, G. Zeng, Y. Cai, X. Wei, Y. Zhou, S. Li, Y. Fang, Y. Zhang, Cd (II) removal from aqueous solution by adsorption on α-ketoglutaric acid-modified magnetic chitosan, Appl. Surf. Sci., 292 (2014) 710–716.
[57] A.Z.M. Badruddoza, Z.B.Z. Shawon, W.J.D. Tay, K. Hidajat, M.S. Uddin, Fe_3O_4/cyclodextrin polymer nanocomposites for selective heavy metals removal from industrial wastewater, Carbohydr. Polym., 91 (2013) 322–332.
[58] X. Xin, Q. Wei, J. Yang, L. Yan, R. Feng, G. Chen, B. Du, H. Li, Highly efficient removal of heavy metal ions by amine-functionalized mesoporous Fe_3O_4 nanoparticles, Chem. Eng. J., 184 (2012) 132–140.
[59] A. Chen, G. Zeng, G. Chen, X. Hu, M. Yan, S. Guan, C. Shang, L. Lu, Z. Zou, G. Xie, Novel thiourea-modified magnetic ion-imprinted chitosan/TiO_2 composite for simultaneous removal of cadmium and 2, 4-dichlorophenol, Chem. Eng. J., 191 (2012) 85–94.
[60] M. Adeli, Y. Yamini, M. Faraji, Removal of copper, nickel and zinc by sodium dodecyl sulphate coated magnetite nanoparticles from water and wastewater samples, Arab. J. Chem., DOI: 10.1016/j.arabjc.2012.10.012.
[61] J. Wang, S. Zheng, Y. Shao, J. Liu, Z. Xu, D. Zhu, Amino-functionalized Fe_3O_4@ SiO_2 core–shell magnetic nanomaterial as a novel adsorbent for aqueous heavy metals removal, J. Colloid Interface Sci., 349 (2010) 293–299.
[62] C.M. Chou, H.L. Lien, Dendrimer-conjugated magnetic nanoparticles for removal of zinc (II) from aqueous solutions, J. Nanopart. Res., 13 (2011) 2099–2107.
[63] C.A.C. Rosas, M. Franzreb, F. Valenzuela, W.H. Höll, Magnetic manganese dioxide as an amphoteric adsorbent for removal of harmful inorganic contaminants from water, React. Funct. Polym., 70 (2010) 516–520.
[64] O. Ozay, S. Ekici, Y. Baran, S. Kubilay, N. Aktas, N. Sahiner, Utilization of magnetic hydrogels in the separation of toxic metal ions from aqueous environments, Desalination, 260 (2010) 57–64.